Development Advance Online Articles. First posted online on 7 August 2015 as 10.1242/dev.122176
Access the most recent version at http://dev.biologists.org/lookup/doi/10.1242/dev.122176

Meis1 coordinates a network of genes implicated in eye development and microphthalmia

Séverine Marcos[1,2], Monica González-Lázaro[3], Leonardo Beccari[1,2], Laura Carramolino[3], Maria Jesus Martin-Bermejo[1,2], Oana Amarie[4], Daniel Mateos-San Martín[3], Carlos Torroja[5], Ozren Bogdanović[6,7], Roisin Doohan[3], Oliver Puk[4], Martin Hrabě de Angelis[4], Jochen Graw[4], Jose Luis Gomez-Skarmeta[6], Fernando Casares[6], Miguel Torres[3*] Paola Bovolenta[1,2*]

[1]Centro de Biología Molecular "Severo Ochoa", CSIC-UAM, [2]CIBER de Enfermedades Raras (CIBERER), c/ Nicolás Cabrera, 1, E-28049 Madrid, Spain. [3]Departamento de Desarrollo y Reparación Cardiovascular, and [5]Bioinformatics Unit, Centro Nacional de Investigaciones Cardiovasculares (CNIC), c/ Melchor Fernández Almagro, 3, E-28029 Madrid, Spain; [4]Institute of Developmental Genetics Helmholtz Center Munich; D-85764 Neuherberg, Germany; [6]Centro Andaluz de Biología del Desarrollo (CABD), CSIC-UPO, Carretera de Utrera Km1, E-41013 Sevilla, Spain; [7]ARC Center of Excellence in Plant Energy Biology, School of Chemistry and Biochemistry, Faculty of Science, The University of Western Australia, Perth, WA 6009, Australia

Key words: Developmental disorders, Notch signalling, patterning, TALE-transcription factors, microphthalmia.

***Co-corresponding authors at:**

Paola Bovolenta
Centro de Biología Molecular Severo Ochoa
CSIC-UAM.
c/ Nicolás Cabrera, 1
28049 Cantoblanco, Madrid. Spain
Tel: 34 91 196 4718 (office)
Fax: 34 91 196 4420
email: pbovolenta@cbm.csic.es

Miguel Torres
Centro de Investigaciones Cardiovasculares
Instituto de Salud Carlos III
c/ Melchor Fernández Almagro, 3,
E-28029 Madrid, Spain
Tel: 34 914531278
Fax: 34 914531240
email: mtorres@cnic.es

Summary

Microphthalmos is a rare congenital anomaly characterized by reduced eye size and visual deficits of variable degrees. Sporadic and hereditary microphthalmos has been associated to heterozygous mutations in genes fundamental for eye development. Yet, many cases are idiopathic or await the identification of molecular causes. Here we show that haploinsufficiency of *Meis1*, a transcription factor with an evolutionary conserved expression in the embryonic trunk, brain and sensory organs, including the eye, causes microphthalmic traits and visual impairment, in adult mice. By combining the analysis of *Meis1* loss-of-function and conditional *Meis1* functional rescue with ChIP-seq and RNA-seq approaches we show that, in contrast to Meis1 preferential association with Hox-Pbx binding sites in the trunk, Meis1 binds to Hox/Pbx-independent sites during optic cup development. In the eye primordium, Meis1 coordinates, in a dose-dependent manner, retinal proliferation and differentiation by regulating genes responsible for human microphthalmia and components the Notch signalling pathway. In addition, Meis1 is required for eye patterning by controlling a set of eye territory-specific transcription factors, so that in *Meis1*$^{-/-}$ embryos boundaries among the different eye territories are shifted or blurred. We thus propose that *Meis1* is at the core of a genetic network implicated in eye patterning/microphthalmia, itself representing an additional candidate for syndromic cases of these ocular malformations.

Introduction

Eye formation initiates with the specification of the retinal field in the anterior neural plate followed by morphogenetic rearrangement of retinal progenitors to form the optic vesicles. Subsequent interaction of the optic neuroepithelium with the surrounding tissue generates the optic cup, which is concomitantly patterned along its three main axes: proximo-distal, naso-temporal and dorso-ventral. This results in the formation of the neural retina, retinal pigment epithelium (RPE), optic stalk and lens (Martinez-Morales et al., 2004), the proliferation and differentiation of which generates a mature eye (Esteve and Bovolenta, 2006). Disruption of any of these events leads to ocular malformations, including anophthalmia (complete absence of the ocular globe) or microphthalmia (significant reduction of the globe axial length), which, in turn, cause severe visual deficits that, for microphthalmia, account for up to 11% of infant blindness in developed countries (Bardakjian and Schneider, 2011).

Cases of anophthalmia and microphthalmia have been associated with homozygous and heterozygous mutations in genes at the core of forebrain regulatory networks (Beccari et al., 2013), such as the transcription factors (TFs) *SOX2* (Fantes et al., 2003), *OTX2* (Ragge et al., 2005), *PAX6* (Glaser et al., 1994), *VSX2/CHX10* (Ferda Percin et al., 2000), *RAX* (Voronina et al., 2004), *FOXE3* (Reis et al., 2010) and perhaps *SIX6* (Gallardo et al., 2004); in key components of cell to cell communication, including *SHH* (Schimmenti et al., 2003) and *BMP4* (Reis et al., 2011), or in genes involved in retinal progenitors' proliferation and survival such as *STRA6* (Pasutto et al., 2007; White et al., 2008), *BCOR* (Ng et al., 2004), *HCCS* (Indrieri et al., 2013; Morleo et al., 2005), and *SMOC1* (Abouzeid et al., 2011; Okada et al., 2011). Yet, only a minor proportion of patients receive accurate molecular diagnosis regarding the pathogenesis of their ocular malformation (Bardakjian and Schneider, 2011; Williamson and FitzPatrick, 2014), indicating that additional causative genes need to be identified. Given that anophthalmia and microphthalmia frequently occur in association with other birth defects, most commonly involving anomalies of the limbs, face, ears and skeletal-muscle system (Slavotinek, 2011), genes implicated in multiple aspects of embryonic development, such as *Meis1*, are good candidates to be explored.

Meis1, its *Drosophila* homolog homothorax (*Hth*) and the related *Meis2* and *Meis3*, belongs to a subfamily of TALE (three amino-acid loop extension) homeodomain-containing TF (Longobardi et al., 2014). Meis proteins form stable heteromeric complexes with other transcriptional regulators, enhancing their affinity and specificity of binding to DNA sites present in the target gene locus (Penkov et al., 2013; Slattery et al., 2011). For example,

together with Pbx1, Meis1 plays a major role as a cofactor for the TFs of the HOX complex, which, in turn, have a pivotal and evolutionary conserved role in orchestrating embryonic trunk development (Duboule, 2007; Mallo and Alonso, 2013). According with this notion, loss of *Meis1* function impairs the formation of *Meis1*-expressing trunk organs and systems, such as the limbs, heart, blood, and vasculature (Azcoitia et al., 2005; Erickson et al., 2010; Hisa et al., 2004; Mercader et al., 1999; Mercader et al., 2009; Zhang et al., 2002).

Members of the *Meis* subfamily are however expressed also in the brain and sensory organs (Schulte and Frank, 2014), which are Hox-free embryonic regions (Duboule, 2007; Mallo and Alonso, 2013). In particular, *Meis1* is expressed in the vertebrate forebrain and sensory organ primordia, including the eye, being essential for the specification of part of these structures. Indeed, genetic inactivation of *Meis1* in mice causes lens reduction and abnormal retinal morphology (Hisa et al., 2004). Cardio-vascular related embryonic lethality of *Meis1*$^{-/-}$ embryos (Azcoitia et al., 2005; Hisa et al., 2004) and virtual lack of information on alternative and Hox-independent transcriptional mechanisms Meis1 must adopt in the head region (Longobardi et al., 2014) have been possible hurdles to understand why and how these eye defects arise.

Here we have begun to address these issues by taking advantage of *Meis1* loss-of-function and conditional *Meis1* functional rescue in mice, combined with ChIPseq and RNAseq approaches. Our results indicate that *Meis1*, by binding to "Meis-only" binding sites on the DNA, regulates (directly and indirectly) the expression of genes involved in patterning, proliferation and differentiation of the neural retina, including components of the Notch signalling pathway. Meis1 also is at the core of a genetic network implicated in mammalian microphthalmia, and its haploinsufficiency suffices to cause microphthalmic traits in adult mice, suggesting that *Meis1* itself represents an additional candidate for this ocular malformation.

Results

Meis1 deficiency causes embryonic microphthalmia

Meis1 is uniformly expressed in the zebrafish and chick eye primordium and progressively retracts from the central retina following the wave of retinal cell differentiation. In both species, *Meis1* regulates the expression *cyclinD1*, thereby promoting G1-S transition of retinal cells and thus the generation of sufficient numbers of retinal progenitors (Bessa et al., 2008;

Heine et al., 2008). Accordingly, interference with *Meis1* expression causes eye hypoplasia (Bessa et al., 2008; Heine et al., 2008).

We reproduced these observations in mice. *Meis1* mRNA localized to the eye field (Fig. 1). Its expression (Fig. 1A-E) and that of its protein (Fig. 1I-K) is thereafter maintained in the optic neuroepithelium and the overlying surface ectoderm throughout eye formation, according to the distribution detected with a LacZ reporter (Hisa et al., 2004). Meis1 expression was also maintained in retinal neurons as defined by its co-expression with the neuronal differentiation marker TuJ1 (Fig. 1L, M). Although *Meis2* has been reported to be transiently expressed in E9.5 optic vesicles (Heine et al., 2008), we could not detect *Meis2* expression at any early stages of eye development (Fig. 1F-H). Thus, early mouse eye development seems to depend mostly on *Meis1* function, in contrast to what observed in zebrafish and chick, in which *Meis2* is instead clearly detected (Bessa et al., 2008; Heine et al., 2008). Complete inactivation of *Meis1* caused lens vesicle reduction, as described using a different *Meis1*$^{-/-}$ mouse line (Hisa et al., 2004) but we did not observe the reported retinal duplication (Hisa et al., 2004). Instead, we noticed a significant reduction of the optic cup compared to wt littermates. This reduction was first apparent at E11 (Fig. 2) and became accentuated with development, especially in the ventral side, so that E13 *Meis1*$^{-/-}$ eyes were roughly half the size of that of wt (Fig. 2S). This was associated with a significant decrease in BrdU incorporation and *cyclinD1* expression (Fig. S1D-F; Fig. 2A-C, T), although there was no statistically significant difference in the mitotic index- calculated as the number of cells in M-phase (pHistoneH3)/area- among wt and *Meis*1 null embryos in both the neural retina and the retina pigmented epithelium (Fig. 2U).

Together these observations indicate that the proposed Hth/Meis1-mediated control of retinal progenitor proliferation is conserved in mice and complete loss of *Meis1* function drastically affects ocular development, causing microphthalmia.

Microphthalmia is associated with decreased neurogenesis and increased apoptosis

Previous studies in *Drosophila* and zebrafish retina have shown that Meis1/Hth expression is turned off in differentiating cells and its forced maintenance prevents the acquisition of a differentiated neuronal fate (Bessa et al., 2002; Bessa et al., 2008). This down-regulation was not observed in the embryonic mouse retina, in which differentiated neurons are still Meis1 positive (Fig. 1M). We thus asked if the reduced eye size of *Meis1* null embryos was also associated to an abnormal neurogenesis.

To explore this possibility, we first compared the onset of Fgf signalling, which triggers retinal neurogenesis (Martinez-Morales et al., 2005), in E11.5 wt and mutant embryos. *Fgf15* was strongly expressed in the wt central retina but was visibly reduced in both level and extension in *Meis1*$^{-/-}$ embryos (Fig. 1G-I). Furthermore, the amount of Otx2+ retinal progenitors (Fig. S1G, I; (Bovolenta et al., 1997) and that of Tuj1+ or Islet1/2+ differentiating neurons (Esteve et al., 2011), was reduced in E12/E13 *Meis1*$^{-/-}$ retinas (Fig. 2J, L, M, O). In contrast to what reported in zebrafish and chick (Bessa et al., 2008; Heine et al., 2008), in *Meis1* null embryos, but not in wt, the prospective neural retina of E12.5-E13.5 embryos showed a significant number of TUNEL and cleaved-Caspase3-positive apoptotic cells (Fig. 1P-R,V). The majority of apoptotic cells were concentrated in the regions of ongoing neuronal differentiation (compare Fig. 2O and R), suggesting a link between the two events.

Haploinsufficiency of *Meis1* causes microphthalmic traits in adult mice

In humans, microphthalmia is often caused by dominant heterozygous mutations, especially when mutations hit genes fundamental for eye development (Williamson and FitzPatrick, 2014). We thus investigated if loss of one *Meis1* allele suffices to impair eye growth. Indeed, the size of the eye in *Meis*$^{+/-}$ embryos was slightly reduced in all of the embryos analysed (30/30) as compared to wt (Fig. 2A,B, D,E, G,H; S) and associated with an evident decrease in *cyclinD1* expression (Fig. 1B). Furthermore, the domain of expression of markers implicated in neuronal differentiation, including *Fgf15*, *Otx2*, *Islet1/2* and TuJ1, was smaller than that observed in wt littermates but not as reduced as that observed in *Meis1*$^{-/-}$ embryos (Fig. 2G-O; Fig. S1G-I). As in homozygous mutants, the retinas of *Meis1*$^{+/-}$ embryos presented an increased number of apoptotic cells in the region of active neurogenesis (Fig. 2Q).

Altogether these observations suggested that heterozygous embryos presented a milder version of the ocular phenotype observed in *Meis1* null mice. To confirm this possibility and exclude that reduced *Meis1* function may simply delay eye development, we asked if the observed embryonic defects persisted into adulthood, as *Meis*$^{+/-}$ mice, in contrast to the homozygous, are viable and fertile.

Scheimpflug imaging revealed no anterior segment abnormality in adult *Meis*$^{+/-}$ animals as compared to wt littermates (Fig. S2). Likewise Optical Coherence Tomography (OCT) showed no defects in the number and distribution of the main blood vessels when adult wt and *Meis1* heterozygous animals were compared (Fig. 3A,B). In contrast, non-invasive

analysis of left and right eye morphometrics and histological analysis of the retina showed that in *Meis1*$^{+/-}$ mice, the axial length of the optic globe and the thickness of the neural retina were significantly decreased (Fig. 3C-H). This reduced thickness seemed to affect, albeit slightly, all nuclear layers (Fig. 3E, F) and could result from the decrease in neurogenesis observed in the heterozygous embryos coupled to the increase in apoptosis. Notably, these morphological changes were associated to a significant loss of visual performance (Fig. 3I), as determined by the virtual drum vision test (Prusky et al., 2004).

Thus, haploinsufficiency of *Meis1* causes morphological and functional defects characteristic of microphthalmia (Williamson and FitzPatrick, 2014). Microphthalmia is likely a direct consequence of Meis1 requirement in the retinal neuroepithelium since blood vessels and lens, which may both influence retinal development, were normally formed.

Microphthalmia is not a consequence of *Meis1* function in the vascular system.

To further confirm the idea that the microphthalmia observed in *Meis1* mutant embryos is independent from the abnormal development of the hematopoietic/vascular system characteristic of *Meis1* null embryos (Azcoitia et al., 2005; Hisa et al., 2004), we analysed a mouse line with a targeted rescue of Meis1 function in the hematopoietic and vascular system in a *Meis1a*$^{-/-}$ background (*Meis1a*$^{-/-}$*;Tie2Cre;R26Meis2a;* (Rosello-Diez et al., 2014).

In contrast to the evident absence of haemorrhage, usually present in *Meis1* null embryos (Fig. 4A-C*;* (Rosello-Diez et al., 2014), the eye size of all of the analysed *Meis1a*$^{-/-}$*;Tie2Cre;R26Meis2a* embryos (13/13) was reduced and comparable to that observed in the *Meis1a*$^{-/-}$*;Tie2Cre* littermates (Fig. 4A-C). Indeed, at E13 the area of the neural retina of *Meis1a*$^{-/-}$*;Tie2Cre;R26Meis2a* and *Meis1a*$^{-/-}$*;Tie2Cre* embryos was, on average and respectively, 47% and 48.2% smaller than that of the *Meis1a*$^{+/+}$*;Tie2Cre;R26Meis2a* control littermates. This reduction is very similar to that observed in the *Meis1*$^{-/-}$ embryos (Fig. 2S). Likewise, in both *Meis1a*$^{-/-}$*;Tie2Cre* and *Meis1a*$^{-/-}$*;Tie2Cre;R26Meis2a* E13.5 retinas, the number of Tuj1+ differentiating neurons was similarly reduced (Fig. 4D-F) and the expression of optic cup patterning markers altered. For example, and as observed in *Meis1* null embryos (Fig. S1J-L; and see below), the distribution of the TF Pax2, normally restricted to cells of the optic disc at E12/13 ((Morcillo et al., 2006); Fig. S1J; Fig. 4G) was instead expanded in the ventral and dorsal retina of both *Meis1a*$^{-/-}$*;Tie2Cre* and *Meis1a*$^{-/-}$*;Tie2Cre;R26Meis2a* embryos (Fig. 4H, I), comparably to what observed in *Meis1* mutant embryos (Fig. S1K, L).

Meis1 interacts with a set of enhancers specifically involved in eye development using Hox/Pbx-independent binding sites

Altogether these data indicate that a full dose of *Meis1* is required for the progression of retina development. Reduced Meis1 levels prevent retinal progenitors from undertaking a normal proliferative and differentiation program, ultimately leading some cells to death. As previously noted (Heine et al., 2008), *cyclinD1* down-regulation by itself can hardly explain this severe phenotype because retinal differentiation is normal in *cyclinD1*$^{-/-}$ mice (Sicinski et al., 1995) and overexpression of *cyclinD1* only partially rescues the effect of loss-of-*Meis1* function (Heine et al., 2008). Thus besides *cyclinD1*, Meis1 likely regulates additional neurogenic pathways. This regulation must take place via a Hox/Pbx-independent mechanism because Hox genes, well known partners of Meis in the trunk, are not expressed in the head (Schulte and Frank, 2014). Furthermore, there is no indication that Pbx genes contribute to early eye formation, although compound knock-out mice have been generated and extensively studied (i.e. (Capellini et al., 2011; Stankunas et al., 2008).

To address this question and identify the binding sites (BS) of endogenous Meis1 protein in the developing eye, we performed ChIPseq analysis using isolated E10.5 optic cups, shortly before the detection of overt *Meis1*$^{-/-}$ eye defects. We identified a total of 5361 Meis1-BS in the genome and a collection of 3182 genes, whose Transcription Start Sites (TSS) were the closest to any Meis1-BS (Supplementary Information). As previously reported (Penkov et al., 2013), most Meis1-BS lied in regions remote from their closest associated TSS (Fig. 5A). To further study the functional relevance of Meis-BS we performed further ChIPseq analysis of the E10.5 optic cup to determine Histone modification marks that identify promoter (H3K4me3) and enhancer regions (H3K4me1). Meis-BS associated very significantly with both H3K4me1 and H3K4me3 marks, indicating a preference for enhancer and promoter region binding (Fig. 5B). When comparing Meis preference for binding to H3K4me1 and H3K4me3 marks, as reported in other tissues (Penkov et al., 2013), we found that Meis1 preferentially binds to enhancer regions (Fig. 5B). Meis selects two main sequences in the embryonic trunk: the Pbx-Hox binding sequence (A/TGATNNAT), to which it binds indirectly, and a direct binding site (TGACAG) (Penkov et al., 2013). To determine binding preferences in the developing eye, we identified consensus sequences in E10.5 eye Meis-BS collection. We found only one consensus sequence showing a unimodal distribution with the maximum mapping to the center of the Meis-BS and therefore representing the Meis1-bound core sequence (m1 sequence, Fig. 5C). We identified three additional consensus sequences showing a bimodal distribution with maxima mapping at a certain distance from

the Meis-BS center, likely representing cooperating sequences not directly bound by Meis1 (m2-m3 in Figure 5C). The m1 consensus is a very close variant of the Meis1 direct binding sequence identified in the trunk (Penkov et al., 2013), whereas m2-m3 sequences were low complexity or rather relaxed sequences that we could not correlate to previously described consensus binding motifs.

The previous results indicated that in the eye Meis1 selects BSs and sequences unrelated to the Hox-Pbx network. In support of this view, the prominent pattern of Meis binding to the HoxA cluster is completely absent in the E10.5 eye (Fig. 5D). We then looked for previously described Meis-regulated enhancers in the developing eye. Within the Meis1-BS collection, we found the previously described Meis-BS in the *Pax6* lens ectoderm enhancer (Zhang et al., 2002) and an additional peak in the *Pax6* third intron, but not the *Pax6*-associated Meis-BS reported after embryonic trunk ChIP-seq (Penkov et al., 2013) or those found in a pancreatic enhancer (Zhang et al., 2006) (Fig. 5E). The eye-specific Meis1-BS coincided with H3K4me1^{high}/H3K4me3^{low} marks typical of enhancer regions (Fig. 5E). Remarkably, despite the distance between Meis1-BS and TSS, the study of "Biological Process" and "Mouse Phenotype" Gene Ontology (GO) classes for the Meis1-BS associated genes identified eye development classes as the most overrepresented, with a predominance of "eye size" and "eye morphology" categories (Fig. 5F). Thus, Meis1 binding profile reveals its functional association with enhancers involved in eye development, at difference with what observed in the embryonic trunk after a similar analysis (Penkov et al., 2013), used here for comparison. Besides "eye development" categories, the "Notch signalling" class appeared enriched in Meis1-BS associated genes (Fig. 5F) with GO analysis.

Meis1 regulates the expression of Notch pathway genes and of selected genes involved in mammalian microphthalmia

To correlate the Meis1-BS pattern with actual gene expression regulation, we compared E10.5 wt and *Meis1*$^{-/-}$ eye-cup transcriptomes by RNA-seq, identifying 406 downregulated and 242 upregulated transcripts (Supplementary Table I, II, III). The expression of transcripts encoding the core factors of the Notch pathway was extensively downregulated in *Meis1* mutants (Fig. 6A), indicating that this pathway is a major target of Meis1 regulation in the developing eye. To determine whether some of the genes coding for core components of the Notch pathway could be direct targets of Meis1, we studied the occurrence of Meis1-BS in the Enhancer-Promoter Units (EPUs) described in the ENCODE project (Shen et al., 2012). We found Meis-BS associated with the enhancer regions of *Notch2*, *Jag1*, *Hes2* and *Hes5*, in

coincidence with enhancer histone marks in the E10.5 eye (Fig. S3). A clear down-regulation of *Hes5* mRNA, a major effector of Notch signalling, was further confirmed by comparative ISH analysis in wt and *Meis1* mutants (Fig. 2D-F). These results suggest Meis1 controls Notch pathway activity at various levels.

In addition, the association of Meis1-BS to genes involved in eye size regulation together with the reduced eye size of *Meis1* mutants further suggested a relationship between Meis1 function and the direct or indirect regulation of microphthalmia genes. RNA-seq analysis focused on 121 mouse genes linked to microphthalmia confirmed this association (Fig. 6B,C). Interestingly, the human orthologs of the five most downregulated genes belonging to this class, *Pitx3, Smoc1*, *Cryba1*, *Cryaa*, and *FoxE3* have been associated to human microphthalmia (Fig. 6C) and a specific survey of all the mouse orthologs of human microphthalmia genes showed a very significant trend to downregulation in *Meis1* mutants (Fig. 6C). These results identify Meis1 as a major regulator of microphthalmia-associated genes. To analyse possible direct targets within genes that change their expression levels, we determined the presence of Meis-BS in the EPUs of the 35 microphthalmia-associated genes that showed the strongest change in expression. We found that 11 out of these 35 genes contained one or more Meis-BS in their EPUs in coincidence with enhancer histone marks in E10.5 eyes (Fig. 6D, S4 and not shown). Interestingly, 12 of the 35 genes showing altered expression and 8 of the 11 genes with Meis1-BS in their EPUs code for TFs, including some of the more frequently associated with human microphthalmia (*Otx2*, *Vsx2*, *Sox2*; Fig. 6D). These results suggest that Meis1 controls eye size at various levels but predominantly by orchestrating the regulation of microphthalmia-associated TFs.

Meis1 is required to sharpen the boundaries among the different eye territories

Because eye development gene classes were overrepresented in Meis1 ChIP-seq analysis (Fig. 5F), developmental processes other than neurogenesis were likely to be affected in *Meis1* mutant eyes. To test this possibility we analysed the distribution of well-established markers of eye patterning. Although most of these markers were detected, their distribution was generally shifted with blurred boundaries: for example, the border between Pax2, a marker of the proximal eye (optic stalk), and Pax6, a marker of the distal eye, was distally shifted, with a clear increase of Pax2 expression in *Meis1* mutants vs wt embryos (Fig. 7A-F), well in agreement with the enhanced expression of Shh in mutants (Fig. 6C), which is known to expand the optic stalk. Similarly, Otx2, a RPE marker (Martinez-Morales et al., 2004), was abnormally extended in the ventro-distal retina (Fig. 7G-I), according to RNA-seq analysis

and the presence of Meis-BSs in its locus (Fig. 6C, D). The *Otx1*+ peripheral retina invaded the *Vsx2*+ central retina (Fig. 7J-O), again in agreement with our "omics" analysis indicating that Meis1 might activate *Vsx2* (Fig. 6C, D). Patterning along the dorso-ventral axis was also abnormal with an expansion of the *Tbx5*+ dorsal region and a reduction of the *Vax2*+ ventral retina, whereas the expression of *FoxD1*, a temporal retinal marker, was considerably reduced (Fig. 7P-X). Notably, blurring of all boundaries was dose-dependent as these defects were milder in *Meis1*$^{+/-}$ eyes.

Discussion

In mammals, *Meis1* is essential for life because its activity is required for the formation of crucial organs: the heart, vasculature and hematopoietic system (Azcoitia et al., 2005; Hisa et al., 2004). During the development of these structures, as well as in that of the limbs, Meis1 acts as a cofactor for Hox proteins, often in cooperation with the related Pbx TFs (Penkov et al., 2013). Our study demonstrates that Meis1 is also crucial for the progressive formation of the eye, but, in this case, its function is mediated by Hox/Pbx-independent BSs on the DNA. In the absence of *Meis1*, the expression of the main patterning determinants of the optic cup is altered and the boundaries between the proximo-distal, dorso-ventral and naso-temporal domains of the cup are shifted or blurred. Retinal neurogenesis is also affected because Meis1, directly or indirectly, controls the expression of components of the neurogenic cascade mediated by the Notch receptor. Furthermore, Meis1 is required for the expression of a set of genes involved in mammalian microphthalmia. Accordingly, *Meis1* haploinsufficient adult mice present morphological and functional defects characteristic of this congenital defect. Therefore, our data, together with previous studies showing that *Meis1* controls lens development and cyclinD1-mediated retinal proliferation (Bessa et al., 2008; Heine et al., 2008; Zhang et al., 2002), indicate that *Meis1* is a global regulator of eye development.

At least in mammals, this key function does not seem to be shared by the related *Meis2* or *Meis3*. *Meis3* is expressed in the eye only when the first RGCs begin to differentiate (Gray et al., 2004). Both *Meis2* and *Meis1* contribute to lens specification by binding to the same BS present in a lens specific enhancer of the *Pax6* locus (Zhang et al., 2002), but only *Meis1* is strongly and continuously expressed in the retinal neuroepithelium, according to our data and the distribution previously reported (Zhang et al., 2002). In consonance, *Meis2*$^{-/-}$

mice have no evident early eye alterations (MT, unpublished observations), suggesting that the reported *Meis2* expression in the optic vesicle (Heine et al., 2008) is either too transient to be always detected and/or dispensable in the gene regulatory network that controls early eye formation. This predominant role of *Meis1* in the mammalian eye primordium differs from that reported in chick or fish, in which alteration of *Meis2* levels also perturbs eye development (Conte et al., 2010; Heine et al., 2008). Furthermore, in contrast to its role, limited to neurogenesis in zebrafish (Bessa et al., 2008), *Meis1* is also critical for patterning and neuronal differentiation in the mouse retina. This latter function is supported by the maintenance of Meis1 expression in the differentiated neurons, which are very reduced in *Meis1*$^{-/-}$ embryos. A similar role has been observed in chick, in which interference with Meis function compromises the appearance of retinal differentiation markers (Heine et al., 2008), including *Foxn4*, a TF directly regulated by Meis1 and important for the generation of horizontal and amacrine neurons (Islam et al., 2013). As shown here, Meis2 rescues Meis1 deficiency in the vascular system, indicating that both proteins are functionally similar and thus any of them could provide the functions required during eye development. Differential evolution of the regulatory elements controlling *Meis1* and *Meis2* expression, rather than Meis1/2 protein functional specialization, may thus underlie their different requirement in fish, avian and mammal eye development.

Our expression and genomic analysis indicates that Meis1 must act quite upstream in the gene regulatory network controlling eye formation, as several of its targets are, themselves, TFs at the core of the network such as Sox2, Otx2 or Pax6 (Beccari et al., 2013). Genetic inactivation of *Meis1* does not prevent the formation of the eye primordium, which has however a fuzzy pattern. This “fuzziness” affects its main tissues- optic stalk, neural retina, RPE- as well as its entire axes, indicating that *Meis1* is crucial to consolidate boundaries among the different eye domains. Meis1 could, for example, render the activity of each one of the tissue determinant genes (i.e. Otx2 for the RPE; (Martinez-Morales et al., 2001)) more efficient. There are different possible and not mutually exclusive mechanisms by which this could occur. In a view molded on its cooperation with Hox/Pbx in the trunk (Duboule, 2007; Penkov et al., 2013), Meis1 could act as a cofactor with a yet-undefined predominant partner, perhaps binding to the m2/m3 core sequence we have identified. This interaction would make the putative factor more efficient allowing correct expression of target genes. Alternatively, Meis1 could interact with a wide variety of TF in the eye, including its own putative targets such as Sox2, Pax6 or Otx2, reinforcing their activity. The latter possibility is supported by the observation that the related Meis2 has been shown to interact at

least with Otx2, Pax3, Pax6 and Pax7 (Agoston et al., 2014; Agoston et al., 2012; Agoston and Schulte, 2009). Alternatively and based on the predominant presence of a "Meis1-only" targeted sequence (m1; Fig. 5) in the eye chromatin, we would like to favor the hypothesis that Meis1 directly binds on enhancers of many determinant genes. Its binding would be necessary to reach sufficient levels of targets' expression, indispensable for regulating the extent of each domain. This possibility could be well illustrated by the possible Meis1 direct regulation of Pax6 in the retina and the establishment of the proximo-distal patterning of the optic vesicle. Indeed, the boundary between the proximal and distal optic vesicle is known to depend on a cross regulatory loop between Pax6, expressed distally, and Pax2 expressed proximally (Schwarz et al., 2000). We have identified a Meis1-BS on a Pax6 enhancer different from that known to mediate lens development (Zhang et al., 2002). In absence of *Meis1*, retinal Pax6 expression is strongly reduced, likely allowing Pax2 up-regulation. This should result in a weak cross-repressive loop between the two TFs and thus in a shifted proximo-distal boundary, indeed observed in *Meis1* mutant embryos. This mechanism could be reinforced by a possible direct repression of Meis1, as we identified ChIP-seq Meis-BS in the *Pax2* locus. Similar considerations could apply for other TFs known to act in a cross-regulatory loop during boundary establishment, as FoxG1 and FoxD1 in the specification of the naso-temporal domains of the retina (Hatini et al., 1994; Huh et al., 1999). Notably, we identified ChIP-seq Meis-BS also in the *FoxD1* locus.

A similar potential direct regulation could also be relevant in the control of components of the Notch signaling pathway, as the Notch2 receptor and the Notch signaling effectors Hes2 and Hes5. For other members of the pathway the decreased expression identified in our RNAseq comparison could be instead indirect. Nevertheless, whether direct or not, the poor Notch pathway activation, in conjunction with a decreased expression of *cyclinD1* and other microphthalmia-associated genes, could explain the *Meis1*$^{-/-}$ microphthalmic phenotype. Indeed, Notch signalling controls the number of progenitors entering retina differentiation: loss of Notch function forestalls retinal neurogenesis (Jadhav et al., 2006), whereas abnormal Notch receptor activation transiently increases retinal proliferation and differentiation (Esteve et al., 2011). Notably, Meis1 action on the Notch pathway and on microphthalmia-related genes could be associated since *Sox1*, *Sox2* and Notch signalling have been shown to regulate each other activity in various contexts (Genethliou et al., 2009; Kan et al., 2004; Neves et al., 2011). Most notably, *Sox2* regulates the Notch signalling pathway in retinal progenitor cells in a concentration-dependent manner,

so that the levels of Sox2 directly correlate with the levels of Notch1 (Taranova et al., 2006), a correlation that we have also observed between *Meis1* levels and *Hes5* expression.

Our RNA-seq analysis reveals a strong association between Meis1 function and genes linked to microphthalmia. As expected by the use of complete E10.5 eye cups, we identified genes expressed only in the lens, such as the TF FoxE3 and the crystalins (Graw, 2009), or in the neural retina, including the TF Vsx2 or Smoc1 (Liu et al., 1994; Okada et al., 2011) or in both, as Sox1/2 or Otx2 (Fuhrmann, 2010; Lang, 2004). This finding not only supports a pleiotropic function of Meis1 in eye formation but also indicates a direct role of Meis1 in the development of the retinal neuroepithelium. Our analysis of mutants with a conditional rescue of *Meis1* expression in the vasculature indicates that the microphthalmia observed is unlikely to derive from abnormal vasculature formation. The relative weight of *Meis1* loss-of-function in the lens or the retina in the microphthalmic phenotype cannot be precisely dissected in our analysis. However, *Meis1* haploinsufficiency in adult mouse eye has no consequence on blood vessel or lens development but it affects the expression of patterning and neurogenic genes, indicating that the retinal neuroepithelium is more sensitive to the levels of *Meis1* expression, demonstrating an important direct implication of *Meis1* in retina development.

In conclusion, our data support that *Meis1* has a critical and previously unreported role in integrating patterning and neurogenesis of the developing eye through the regulation of signalling pathways and patterning genes. More importantly, *Meis1* seems to be at the core of a genetic network implicated in human microphthalmia, itself representing an additional candidate for syndromic cases associated with this ocular malformation. In this respect, eye developmental defects, including bilateral microphthalmia, have been linked to alterations in chromosome 2 (Waters et al., 1993; Weaver et al., 1991), in a region that may include the extensive *MEIS1* regulatory region (Royo et al., 2012), opening the possibility that reduced MEIS1 levels could contribute to the phenotypic traits.

Materials and Methods

Animals. *Meis1a* heterozygous mice were generated as described (Azcoitia et al., 2005). Embryos were obtained from timed (vaginal plug as E0.5) mating of *Meis1a*$^{+/-}$ mice or outbreed CD1 mice. Animals were treated according to institutional or national guidelines for the use of animals in scientific research.

BrdU Incorporation. BrdU (50µg/g body weight of 10mg/ml BrdU) was injected into pregnant mice intraperitoneally. Embryos were sacrificed and collected 1h later.

TUNEL. Staining was performed using the In Situ Cell Death detection kit (Roche) on cryosections following the manufacturer's instructions.

In situ hybridization. E10.5-13.5 embryos were immersion-fixed in 4% paraformaldehyde (PFA)/phosphate buffer for 3h. Tissue was processed for cryo-sectioning in the frontal or horizontal plane and ISH was performed as described (Causeret et al., 2004). The following digoxigenin-labelled mouse specific antisense riboprobes were used: *Fgf15*, *CyclinD1*, *Hes5*, *Tbx5*, *Vax2*, *Foxd1*, *Otx1*, *Vsx2*.

Immunohistochemistry. Cryosections were incubated with 0,1% Triton X-100 in PBS (PBT) and immunofluorescence was performed in PBT with 1% normal goat serum. For Otx2, Pax6 and Pax2 staining, sections were boiled at 110ºC for 2 min in 10mM citrate buffer using a decloaking chamber (Biocare Medical). The following primary antibodies were used: a) Rabbit: anti-meis1a/2a (1:1000, (Mercader et al., 2005), anti-Otx2 (1:1000, Abcam), anti-cleaved Caspase3 (1:1000, Cell Signaling), anti-Pax2 (1:1000, Invitrogen), anti-Pax6 (1:1000, Covance) b) Mouse: anti-phospho-histoneH3 (1:1000, Millipore), anti-BrdU (1:4000) and anti-Islet1/2 (1:500, DSHB 39.4D5), anti-βIII-tubulin (TUJ1) (1:1000, Promega). Secondary antibodies conjugated to Alexa 488 or Alexa 594 (1:1000; Molecular probes) and DAPI (1 µg/ml, Vector) counterstaining were used.

RNA-seq. For RNA-Seq library production, RNA of intact E10.5 optic cups (thus including the lens) from 8 homozygous and wt embryos (out of 41 embryos from 7 litters) was isolated using standard procedures, quantified (260 nm in a NanoDrop) and checked for integrity (Agilent Bioanalyzer; Santa Clara, CA). Total RNA was processed with the TruSeq RNA Sample Preparation v2 Kit (Illumina, San Diego, CA) to construct index-tagged cDNA libraries. The quality, quantity and the size distribution of the Illumina libraries were determined using the DNA-1000 Kit (Agilent Bioanalyzer). Prepared cDNA libraries were applied to an Illumina flow cell for cluster generation (True Seq SR Cluster Kit V2 cBot) and

sequence-by-synthesis single reads of 75b length using the TruSeq SBS Kit v5 (Illumina) were generated on the Genome Analyzer IIx following the standard RNA sequencing protocol. Sequencing adaptor contaminations were removed from reads using cutadapt software (http://code.google.com/p/cutadapt/) and the resulting reads were mapped and quantified on the transcriptome (Ensembl gene-build 70) using RSEM v1.2.3 (Li and Dewey, 2011). Only genes with at least 5 counts per million in at least one sample were considered for statistical analysis. Data were then normalized and differential expression tested using the bioconductor package EdgeR (Robinson et al., 2010). Genes were considered differentially expressed when presented a fold change ≥40%. Data were analyzed using Gene set enrichment and Ingenuity pathways softwares (Biobase International). Mouse microphthalmia genes were obtained by searching the Jackson Laboratory Mouse Genome Informatics database for the term "microphthalmia" in the field "Mouse phenotypes&Mouse models of human disease" of the "Genes and Markers" query. Data are deposited in the NCBI GEO database (accession number GSE62786).

ChIP-seq. ChIP assays to determine the histone methylation marks were performed collecting about 100 eyes from E10.5 mouse embryos. Chromatin was cross-linked with 1% formaldehyde for 15 min and fragmented to obtain DNA in the range of 200–500 bp. DNA was divided in three pools (10µg) and precipitated with 2µg anti-H3K4me1 (CS-037-100, Diagenode), anti-H3K4me3 (pAB-033-050 Diagenode). Immunoprecipitated DNA was purified with QIAquick columns (Qiagen). Data have been deposited in the NCBI GEO database (accession number TO BE INCLUDED). ChIP data for Meis1 were obtained from about 200 eyes of E10.5 CD1 embryos. Two pools of approximately 20µg of total chromatin were immunprecipitated with 4gr of anti-Meis1 antibody (REF) and the immunoprecipitated DNA were purified pooled together. ChIP-seq and bioinformatic processing were performed as described (Penkov et al., 2013). Chromatin was cross-linked with 1% formaldehyde for 15 min and fragmented to 300-500 bp. Data have been deposited in the NCBI GEO database (accession number GSE62786). Annotation of Meis1 BS and identification of Meis1-BS associated genes or over-representation in Gene Ontology and Phenotype association databases was performed with the "Genomic Regions Enrichment of Annotations Tool" (GREAT) (McLean et al., 2010). For the identified peaks, ***de novo motif discovery*** was run to identify consensus sequences enriched in the selected regions versus the whole genome using rGADEM (Li, 2009).

Morphometric and functional analysis of the eye. The visual acuity and the eye morphology of the Meis1a mice were evaluated at 15 weeks of age by Virtual optokinetic drum (Benkner et al., 2013), Scheimpflug Imaging, Optical Coherence Tomography (OCT), and Laser Interference Biometry (LIB). For LIB and OCT, the eyes were treated with 1% atropine to ensure pupil dilation and mice were further anaesthetized with 137 mg ketamine and 6.6 mg xylazine per kg body weight. For all tests previously published protocols were followed: Virtual drum vision test (Prusky et al., 2004); Scheimpflug imaging (Puk et al., 2013a); OCT (Puk et al., 2013b) and LIB (Puk et al., 2006).

Quantifications and statistical analysis: Area measurements and cell counting was performed with a Leica fluorescent microscope and a Leica camera. All statistical analysis was performed using a minimum of 3/6 embryos/eyes per genotype, using ImageJ software. Differences between calculated averages were considered significant when $P<0,05$ using a Student's *t*-test. For each one of the ISH probes or IC markers used in this study, analysis was performed on a minimum of 3 embryos for each genotype. For each embryo, all the sections from both eyes were photographed and compared using sections at the same axial level.

Acknowledgments

We thank JR Martinez-Morales (CBD) for critical reading the manuscript. We are grateful to V. García for mouse care; CMBSO Genomics Facility for help with ChIP-seq and M.J. Gómez-Rodriguez, Manuel Gómez and F. Sánchez-Cabo (CNIC) for bioinformatics analyses. The CNIC Genomics unit performed the RNA sequencing procedures. This work was supported by grants from the Spanish MINECO (BFU2010-16031; BFU2013-43213-P, supported by FEDER Funds), the CIBERER, ISCIII to PB and an Institutional Grant from the Fundación Ramon Areces; by MINECO (BFU2012-31086) and ISCIII (RD12/0019/0005) to MT and S2010/BMD-2315 from CAM to PB and MT; by MINECO (BFU2013-41322-P) and Andalusian Government (BIO-396) to JLG-S and by BFU2014-55738-REDT to PB, JLGS and FC. M.G-L was supported by a grant from the CONACyT. O.B. is supported by an Australian Res. Council Discovery Early Career Researcher Award-DECRA (DE140101962). The CNIC is supported by the MINECO and the Pro-CNIC Foundation.

Author Contributions

PB, MT and SM conceived the study; JG and MHA conceived the phenotypic tests; SM, MGL, LB, LC, RD, OP, OA and MJMB performed experiments; SM, LB, OM, JG, DS-SM, CT, JT, JLGS, FC, MT and PB analysed the data; MT and PB wrote the paper. All authors approved the manuscript.

References

Abouzeid, H., Boisset, G., Favez, T., Youssef, M., Marzouk, I., Shakankiry, N., Bayoumi, N., Descombes, P., Agosti, C., Munier, F. L. et al. (2011). Mutations in the SPARC-related modular calcium-binding protein 1 gene, SMOC1, cause waardenburg anophthalmia syndrome. *American journal of human genetics* **88**, 92-8.

Agoston, Z., Heine, P., Brill, M. S., Grebbin, B. M., Hau, A. C., Kallenborn-Gerhardt, W., Schramm, J., Gotz, M. and Schulte, D. (2014). Meis2 is a Pax6 co-factor in neurogenesis and dopaminergic periglomerular fate specification in the adult olfactory bulb. *Development* **141**, 28-38.

Agoston, Z., Li, N., Haslinger, A., Wizenmann, A. and Schulte, D. (2012). Genetic and physical interaction of Meis2, Pax3 and Pax7 during dorsal midbrain development. *BMC developmental biology* **12**, 10.

Agoston, Z. and Schulte, D. (2009). Meis2 competes with the Groucho co-repressor Tle4 for binding to Otx2 and specifies tectal fate without induction of a secondary midbrain-hindbrain boundary organizer. *Development* **136**, 3311-22.

Azcoitia, V., Aracil, M., Martinez, A. C. and Torres, M. (2005). The homeodomain protein Meis1 is essential for definitive hematopoiesis and vascular patterning in the mouse embryo. *Developmental biology* **280**, 307-20.

Bardakjian, T. M. and Schneider, A. (2011). The genetics of anophthalmia and microphthalmia. *Current opinion in ophthalmology* **22**, 309-13.

Beccari, L., Marco-Ferreres, R. and Bovolenta, P. (2013). The logic of gene regulatory networks in early vertebrate forebrain patterning. *Mech Dev* **130**, 95-111.

Benkner, B., Mutter, M., Ecke, G. and Munch, T. A. (2013). Characterizing visual performance in mice: an objective and automated system based on the optokinetic reflex. *Behavioral neuroscience* **127**, 788-96.

Bessa, J., Gebelein, B., Pichaud, F., Casares, F. and Mann, R. S. (2002). Combinatorial control of Drosophila eye development by eyeless, homothorax, and teashirt. *Genes & development* **16**, 2415-27.

Bessa, J., Tavares, M. J., Santos, J., Kikuta, H., Laplante, M., Becker, T. S., Gomez-Skarmeta, J. L. and Casares, F. (2008). meis1 regulates cyclin D1 and c-myc expression, and controls the proliferation of the multipotent cells in the early developing zebrafish eye. *Development* **135**, 799-803.

Bovolenta, P., Mallamaci, A., Briata, P., Corte, G. and Boncinelli, E. (1997). Implication of OTX2 in pigment epithelium determination and neural retina differentiation. *The Journal of neuroscience : the official journal of the Society for Neuroscience* **17**, 4243-52.

Capellini, T. D., Zappavigna, V. and Selleri, L. (2011). Pbx homeodomain proteins: TALEnted regulators of limb patterning and outgrowth. *Developmental dynamics : an official publication of the American Association of Anatomists* **240**, 1063-86.

Causeret, F., Hidalgo-Sanchez, M., Fort, P., Backer, S., Popoff, M. R., Gauthier-Rouviere, C. and Bloch-Gallego, E. (2004). Distinct roles of Rac1/Cdc42 and Rho/Rock for axon outgrowth and nucleokinesis of precerebellar neurons toward netrin 1. *Development* **131**, 2841-52.

Consortium, T. E. (2012). An integrated encyclopedia of DNA elements in the human genome. *Nature* **489**, 57-74.

Conte, I., Carrella, S., Avellino, R., Karali, M., Marco-Ferreres, R., Bovolenta, P. and Banfi, S. (2010). miR-204 is required for lens and retinal development via Meis2 targeting. *Proceedings of the National Academy of Sciences of the United States of America* **107**, 15491-6.

Duboule, D. (2007). The rise and fall of Hox gene clusters. *Development* **134**, 2549-60.

Erickson, T., French, C. R. and Waskiewicz, A. J. (2010). Meis1 specifies positional information in the retina and tectum to organize the zebrafish visual system. *Neural development* **5**, 22.

Esteve, P. and Bovolenta, P. (2006). Secreted inducers in vertebrate eye development: more functions for old morphogens. *Curr Opin Neurobiol* **16**, 13-9.

Esteve, P., Sandonis, A., Cardozo, M., Malapeira, J., Ibanez, C., Crespo, I., Marcos, S., Gonzalez-Garcia, S., Toribio, M. L., Arribas, J. et al. (2011). SFRPs act as negative modulators of ADAM10 to regulate retinal neurogenesis. *Nature neuroscience* **14**, 562-9.

Fantes, J., Ragge, N. K., Lynch, S. A., McGill, N. I., Collin, J. R., Howard-Peebles, P. N., Hayward, C., Vivian, A. J., Williamson, K., van Heyningen, V. et al. (2003). Mutations in SOX2 cause anophthalmia. *Nature genetics* **33**, 461-3.

Ferda Percin, E., Ploder, L. A., Yu, J. J., Arici, K., Horsford, D. J., Rutherford, A., Bapat, B., Cox, D. W., Duncan, A. M., Kalnins, V. I. et al. (2000). Human microphthalmia associated with mutations in the retinal homeobox gene CHX10. *Nature genetics* **25**, 397-401.

Fuhrmann, S. (2010). Eye morphogenesis and patterning of the optic vesicle. *Current topics in developmental biology* **93**, 61-84.

Gallardo, M. E., Rodriguez De Cordoba, S., Schneider, A. S., Dwyer, M. A., Ayuso, C. and Bovolenta, P. (2004). Analysis of the developmental SIX6 homeobox gene in patients with anophthalmia/microphthalmia. *American journal of medical genetics. Part A* **129A**, 92-4.

Genethliou, N., Panayiotou, E., Panayi, H., Orford, M., Mean, R., Lapathitis, G., Gill, H., Raoof, S., De Gasperi, R., Elder, G. et al. (2009). SOX1 links the function of neural patterning and Notch signalling in the ventral spinal cord during the neuron-glial fate switch. *Biochemical and biophysical research communications* **390**, 1114-20.

Glaser, T., Jepeal, L., Edwards, J. G., Young, S. R., Favor, J. and Maas, R. L. (1994). PAX6 gene dosage effect in a family with congenital cataracts, aniridia, anophthalmia and central nervous system defects. *Nature genetics* **7**, 463-71.

Graw, J. (2009). Mouse models of cataract. *Journal of genetics* **88**, 469-86.

Gray, P. A., Fu, H., Luo, P., Zhao, Q., Yu, J., Ferrari, A., Tenzen, T., Yuk, D. I., Tsung, E. F., Cai, Z. et al. (2004). Mouse brain organization revealed through direct genome-scale TF expression analysis. *Science* **306**, 2255-7.

Hatini, V., Tao, W. and Lai, E. (1994). Expression of winged helix genes, BF-1 and BF-2, define adjacent domains within the developing forebrain and retina. *Journal of neurobiology* **25**, 1293-309.

Heine, P., Dohle, E., Bumsted-O'Brien, K., Engelkamp, D. and Schulte, D. (2008). Evidence for an evolutionary conserved role of homothorax/Meis1/2 during vertebrate retina development. *Development* **135**, 805-11.

Hisa, T., Spence, S. E., Rachel, R. A., Fujita, M., Nakamura, T., Ward, J. M., Devor-Henneman, D. E., Saiki, Y., Kutsuna, H., Tessarollo, L. et al. (2004). Hematopoietic, angiogenic and eye defects in Meis1 mutant animals. *The EMBO journal* **23**, 450-9.

Huh, S., Hatini, V., Marcus, R. C., Li, S. C. and Lai, E. (1999). Dorsal-ventral patterning defects in the eye of BF-1-deficient mice associated with a restricted loss of shh expression. *Developmental biology* **211**, 53-63.

Indrieri, A., Conte, I., Chesi, G., Romano, A., Quartararo, J., Tate, R., Ghezzi, D., Zeviani, M., Goffrini, P., Ferrero, I. et al. (2013). The impairment of HCCS leads to MLS syndrome by activating a non-canonical cell death pathway in the brain and eyes. *EMBO molecular medicine* **5**, 280-93.

Islam, M. M., Li, Y., Luo, H., Xiang, M. and Cai, L. (2013). Meis1 regulates Foxn4 expression during retinal progenitor cell differentiation. *Biology open* **2**, 1125-36.

Jadhav, A. P., Cho, S. H. and Cepko, C. L. (2006). Notch activity permits retinal cells to progress through multiple progenitor states and acquire a stem cell property. *Proceedings of the National Academy of Sciences of the United States of America* **103**, 18998-9003.

Kan, L., Israsena, N., Zhang, Z., Hu, M., Zhao, L. R., Jalali, A., Sahni, V. and Kessler, J. A. (2004). Sox1 acts through multiple independent pathways to promote neurogenesis. *Developmental biology* **269**, 580-94.

Lang, R. A. (2004). Pathways regulating lens induction in the mouse. *The International journal of developmental biology* **48**, 783-91.

Li, B. and Dewey, C. N. (2011). RSEM: accurate transcript quantification from RNA-Seq data with or without a reference genome. *BMC bioinformatics* **12**, 323.

Li, L. (2009). GADEM: a genetic algorithm guided formation of spaced dyads coupled with an EM algorithm for motif discovery. *Journal of computational biology : a journal of computational molecular cell biology* **16**, 317-29.

Liu, I. S., Chen, J. D., Ploder, L., Vidgen, D., van der Kooy, D., Kalnins, V. I. and McInnes, R. R. (1994). Developmental expression of a novel murine homeobox gene (Chx10): evidence for roles in determination of the neuroretina and inner nuclear layer. *Neuron* **13**, 377-93.

Longobardi, E., Penkov, D., Mateos, D., De Florian, G., Torres, M. and Blasi, F. (2014). Biochemistry of the tale transcription factors PREP, MEIS, and PBX in vertebrates. *Developmental dynamics : an official publication of the American Association of Anatomists* **243**, 59-75.

Mallo, M. and Alonso, C. R. (2013). The regulation of Hox gene expression during animal development. *Development* **140**, 3951-63.

Martinez-Morales, J. R., Del Bene, F., Nica, G., Hammerschmidt, M., Bovolenta, P. and Wittbrodt, J. (2005). Differentiation of the vertebrate retina is coordinated by an FGF signaling center. *Dev Cell* **8**, 565-74.

Martinez-Morales, J. R., Rodrigo, I. and Bovolenta, P. (2004). Eye development: a view from the retina pigmented epithelium. *Bioessays* **26**, 766-77.

Martinez-Morales, J. R., Signore, M., Acampora, D., Simeone, A. and Bovolenta, P. (2001). Otx genes are required for tissue specification in the developing eye. *Development* **128**, 2019-30.

McLean, C. Y., Bristor, D., Hiller, M., Clarke, S. L., Schaar, B. T., Lowe, C. B., Wenger, A. M. and Bejerano, G. (2010). GREAT improves functional interpretation of cis-regulatory regions. *Nature biotechnology* **28**, 495-501.

Mercader, N., Leonardo, E., Azpiazu, N., Serrano, A., Morata, G., Martinez, C. and Torres, M. (1999). Conserved regulation of proximodistal limb axis development by Meis1/Hth. *Nature* **402**, 425-9.

Mercader, N., Selleri, L., Criado, L. M., Pallares, P., Parras, C., Cleary, M. L. and Torres, M. (2009). Ectopic Meis1 expression in the mouse limb bud alters P-D patterning in a Pbx1-independent manner. *The International journal of developmental biology* **53**, 1483-94.

Mercader, N., Tanaka, E. M. and Torres, M. (2005). Proximodistal identity during vertebrate limb regeneration is regulated by Meis homeodomain proteins. *Development* **132**, 4131-42.

Morcillo, J., Martinez-Morales, J. R., Trousse, F., Fermin, Y., Sowden, J. C. and Bovolenta, P. (2006). Proper patterning of the optic fissure requires the sequential activity of BMP7 and SHH. *Development* **133**, 3179-90.

Morleo, M., Pramparo, T., Perone, L., Gregato, G., Le Caignec, C., Mueller, R. F., Ogata, T., Raas-Rothschild, A., de Blois, M. C., Wilson, L. C. et al. (2005). Microphthalmia with linear skin defects (MLS) syndrome: clinical, cytogenetic, and molecular characterization of 11 cases. *American journal of medical genetics. Part A* **137**, 190-8.

Neves, J., Parada, C., Chamizo, M. and Giraldez, F. (2011). Jagged 1 regulates the restriction of Sox2 expression in the developing chicken inner ear: a mechanism for sensory organ specification. *Development* **138**, 735-44.

Ng, D., Thakker, N., Corcoran, C. M., Donnai, D., Perveen, R., Schneider, A., Hadley, D. W., Tifft, C., Zhang, L., Wilkie, A. O. et al. (2004). Oculofaciocardiodental and Lenz microphthalmia syndromes result from distinct classes of mutations in BCOR. *Nature genetics* **36**, 411-6.

Okada, I., Hamanoue, H., Terada, K., Tohma, T., Megarbane, A., Chouery, E., Abou-Ghoch, J., Jalkh, N., Cogulu, O., Ozkinay, F. et al. (2011). SMOC1 is essential for ocular and limb development in humans and mice. *American journal of human genetics* **88**, 30-41.

Pasutto, F., Sticht, H., Hammersen, G., Gillessen-Kaesbach, G., Fitzpatrick, D. R., Nurnberg, G., Brasch, F., Schirmer-Zimmermann, H., Tolmie, J. L., Chitayat, D. et al. (2007). Mutations in STRA6 cause a broad spectrum of malformations including anophthalmia, congenital heart defects, diaphragmatic hernia, alveolar capillary dysplasia, lung hypoplasia, and mental retardation. *American journal of human genetics* **80**, 550-60.

Penkov, D., Mateos San Martin, D., Fernandez-Diaz, L. C., Rossello, C. A., Torroja, C., Sanchez-Cabo, F., Warnatz, H. J., Sultan, M., Yaspo, M. L., Gabrieli, A. et al. (2013). Analysis of the DNA-binding profile and function of TALE homeoproteins reveals their specialization and specific interactions with Hox genes/proteins. *Cell reports* **3**, 1321-33.

Prusky, G. T., Alam, N. M., Beekman, S. and Douglas, R. M. (2004). Rapid quantification of adult and developing mouse spatial vision using a virtual optomotor system. *Invest Ophthalmol Vis Sci* **45**, 4611-6.

Puk, O., Dalke, C., Favor, J., de Angelis, M. H. and Graw, J. (2006). Variations of eye size parameters among different strains of mice. *Mamm Genome* **17**, 851-7.

Puk, O., de Angelis, M. H. and Graw, J. (2013a). Lens density tracking in mice by Scheimpflug imaging. *Mamm Genome* **24**, 295-302.

Puk, O., de Angelis, M. H. and Graw, J. (2013b). Longitudinal fundus and retinal studies with SD-OCT: a comparison of five mouse inbred strains. *Mamm Genome* **24**, 198-205.

Ragge, N. K., Brown, A. G., Poloschek, C. M., Lorenz, B., Henderson, R. A., Clarke, M. P., Russell-Eggitt, I., Fielder, A., Gerrelli, D., Martinez-Barbera, J. P. et al. (2005). Heterozygous mutations of OTX2 cause severe ocular malformations. *American journal of human genetics* **76**, 1008-22.

Reis, L. M., Tyler, R. C., Schilter, K. F., Abdul-Rahman, O., Innis, J. W., Kozel, B. A., Schneider, A. S., Bardakjian, T. M., Lose, E. J., Martin, D. M. et al. (2011). BMP4 loss-of-function mutations in developmental eye disorders including SHORT syndrome. *Human genetics* **130**, 495-504.

Reis, L. M., Tyler, R. C., Schneider, A., Bardakjian, T., Stoler, J. M., Melancon, S. B. and Semina, E. V. (2010). FOXE3 plays a significant role in autosomal recessive microphthalmia. *American journal of medical genetics. Part A* **152A**, 582-90.

Robinson, M. D., McCarthy, D. J. and Smyth, G. K. (2010). edgeR: a Bioconductor package for differential expression analysis of digital gene expression data. *Bioinformatics* **26**, 139-40.

Rosello-Diez, A., Arques, C. G., Delgado, I., Giovinazzo, G. and Torres, M. (2014). Diffusible signals and epigenetic timing cooperate in late proximo-distal limb patterning. *Development* **141**, 1534-43.

Royo, J. L., Bessa, J., Hidalgo, C., Fernandez-Minan, A., Tena, J. J., Roncero, Y., Gomez-Skarmeta, J. L. and Casares, F. (2012). Identification and analysis of conserved cis-regulatory regions of the MEIS1 gene. *PloS one* **7**, e33617.

Schimmenti, L. A., de la Cruz, J., Lewis, R. A., Karkera, J. D., Manligas, G. S., Roessler, E. and Muenke, M. (2003). Novel mutation in sonic hedgehog in non-syndromic colobomatous microphthalmia. *American journal of medical genetics. Part A* **116A**, 215-21.

Schulte, D. and Frank, D. (2014). TALE transcription factors during early development of the vertebrate brain and eye. *Developmental dynamics : an official publication of the American Association of Anatomists* **243**, 99-116.

Schwarz, M., Cecconi, F., Bernier, G., Andrejewski, N., Kammandel, B., Wagner, M. and Gruss, P. (2000). Spatial specification of mammalian eye territories by reciprocal transcriptional repression of Pax2 and Pax6. *Development* **127**, 4325-34.

Shen, Y., Yue, F., McCleary, D. F., Ye, Z., Edsall, L., Kuan, S., Wagner, U., Dixon, J., Lee, L., Lobanenkov, V. V. et al. (2012). A map of the cis-regulatory sequences in the mouse genome. *Nature* **488**, 116-20.

Sicinski, P., Donaher, J. L., Parker, S. B., Li, T., Fazeli, A., Gardner, H., Haslam, S. Z., Bronson, R. T., Elledge, S. J. and Weinberg, R. A. (1995). Cyclin D1 provides a link between development and oncogenesis in the retina and breast. *Cell* **82**, 621-30.

Slattery, M., Riley, T., Liu, P., Abe, N., Gomez-Alcala, P., Dror, I., Zhou, T., Rohs, R., Honig, B., Bussemaker, H. J. et al. (2011). Cofactor binding evokes latent differences in DNA binding specificity between Hox proteins. *Cell* **147**, 1270-82.

Slavotinek, A. M. (2011). Eye development genes and known syndromes. *Molecular genetics and metabolism* **104**, 448-56.

Stankunas, K., Shang, C., Twu, K. Y., Kao, S. C., Jenkins, N. A., Copeland, N. G., Sanyal, M., Selleri, L., Cleary, M. L. and Chang, C. P. (2008). Pbx/Meis deficiencies demonstrate multigenetic origins of congenital heart disease. *Circulation research* **103**, 702-9.

Taranova, O. V., Magness, S. T., Fagan, B. M., Wu, Y., Surzenko, N., Hutton, S. R. and Pevny, L. H. (2006). SOX2 is a dose-dependent regulator of retinal neural progenitor competence. *Genes & development* **20**, 1187-202.

Voronina, V. A., Kozhemyakina, E. A., O'Kernick, C. M., Kahn, N. D., Wenger, S. L., Linberg, J. V., Schneider, A. S. and Mathers, P. H. (2004). Mutations in the human RAX homeobox gene in a patient with anophthalmia and sclerocornea. *Human molecular genetics* **13**, 315-22.

Waters, B. L., Allen, E. F., Gibson, P. C. and Johnston, T. (1993). Autopsy findings in a severely affected infant with a 2q terminal deletion. *American journal of medical genetics* **47**, 1099-103.

Weaver, R. G., Rao, N., Thomas, I. T. and Pettenati, M. J. (1991). De novo inv(2)(p21q31) associated with isolated bilateral microphthalmia and cataracts. *American journal of medical genetics* **40**, 509-12.

White, T., Lu, T., Metlapally, R., Katowitz, J., Kherani, F., Wang, T. Y., Tran-Viet, K. N. and Young, T. L. (2008). Identification of STRA6 and SKI sequence variants in patients with anophthalmia/microphthalmia. *Molecular vision* **14**, 2458-65.

Williamson, K. A. and FitzPatrick, D. R. (2014). The genetic architecture of microphthalmia, anophthalmia and coloboma. *European journal of medical genetics* **57**, 369-80.

Zhang, X., Friedman, A., Heaney, S., Purcell, P. and Maas, R. L. (2002). Meis homeoproteins directly regulate Pax6 during vertebrate lens morphogenesis. *Genes & development* **16**, 2097-107.

Zhang, X., Rowan, S., Yue, Y., Heaney, S., Pan, Y., Brendolan, A., Selleri, L. and Maas, R. L. (2006). Pax6 is regulated by Meis and Pbx homeoproteins during pancreatic development. *Developmental biology* **300**, 748-57.

Figures

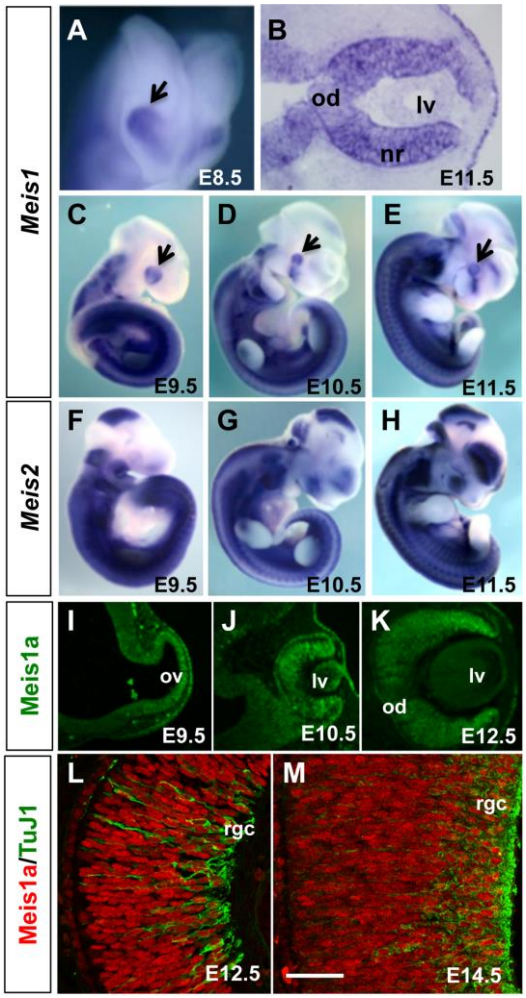

Figure 1. Embryonic expression of *Meis1* and *Meis2*. Frontal (A) and lateral (C-H) view of mouse embryos at stages comprised between E8.5 and E11.5 (as indicated in the panels) hybridized in toto with probes specific for *Meis1* and *Meis2*. B) Frontal paraffin section through the optic cup of an E11.5 mouse embryo hybridized with a probe against *Meis1*. Note that *Meis1* is strongly expressed in the eye field (arrow in A) and its expression is maintained as the optic cup forms (arrows in C-E). The expression is particularly abundant is the neural retina (nr, B). Meis2 is not expressed in the developing eye (F-H) but it is strongly expressed in the mesencephalon and spinal cord. I-M) Frontal cryostat sections of mouse embryos at stages comprised between E9.5 and E14.5 (as indicated in the panels) were immunostained with antibodies against Meis1a, one of the Meis1 isoforms, or co-immunostained with the neuronal differentiation marker TuJ1 (L, M). Note that the protein is detected in the entire optic vesicle and overlying ectoderm, in the developing optic cup and in differentiated neurons. Abbreviations: lv, lens vesicle; nr, neural retina; od, optic disc; ov, optic vesicle, rgc, retinal ganglion cells. Scale bar, 25 μm.

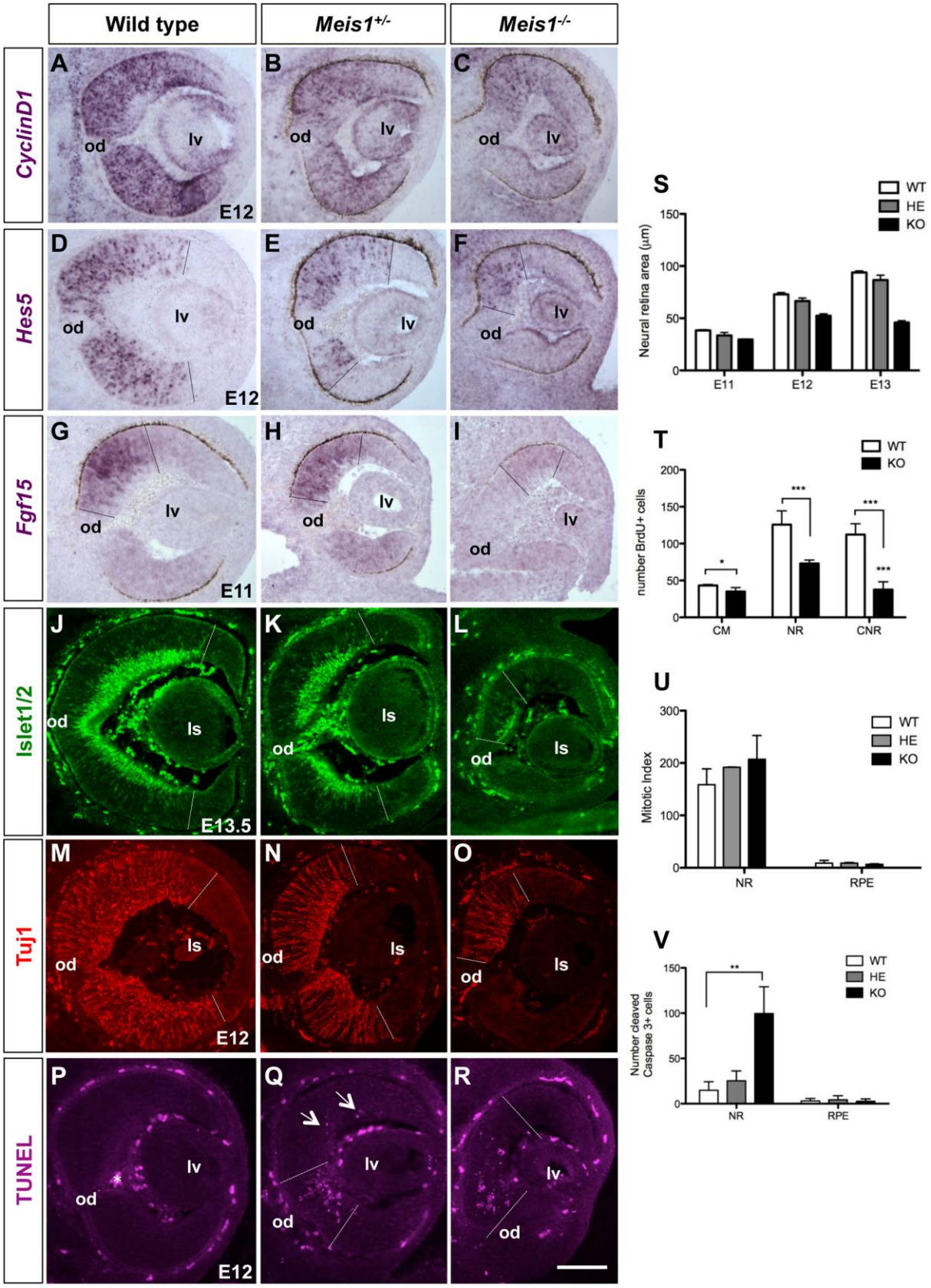

Figure 2. ***Meis1*-loss-of-function causes dose-dependent alterations in retinal neurogenesis leading to microphthalmia**. **A-R**) Frontal sections of E11-13 wt or *Meis1*$^{+/-}$ and *Meis1*$^{-/-}$ optic cups processed for the markers indicated in the panels. Note the decreased

proliferation (less *cyclinD1* expression, B, C) and the impaired onset (*Fgf15*, *Hes5*) and progression (Islet1/2, TuJ1) of neuronal differentiation in *Meis1* mutants associated to increased apoptosis (P-R). Absence of one *Meis1* allele suffices to induce these defects. Dotted lines delineate the extent of marker staining. **S-V**) Quantification of the area (S) BrdU+ (T) PHH3+mitotic (U) and cleaved-Caspase3+ (V) cells in E12.5 optic cups. Total areas were determined using DAPI stained sections. Error bars are standard error of the mean of counting all sections from both eyes of at least 3 different embryos (n=3). There is no statistical difference in the Mitotic Index of the different genotypes (U). *P<0.05. **P<0.01. ***P<0.001. Abbreviations: ls, lens; lv, lens vesicle; od, optic disc. Scale bar, 25 μm.

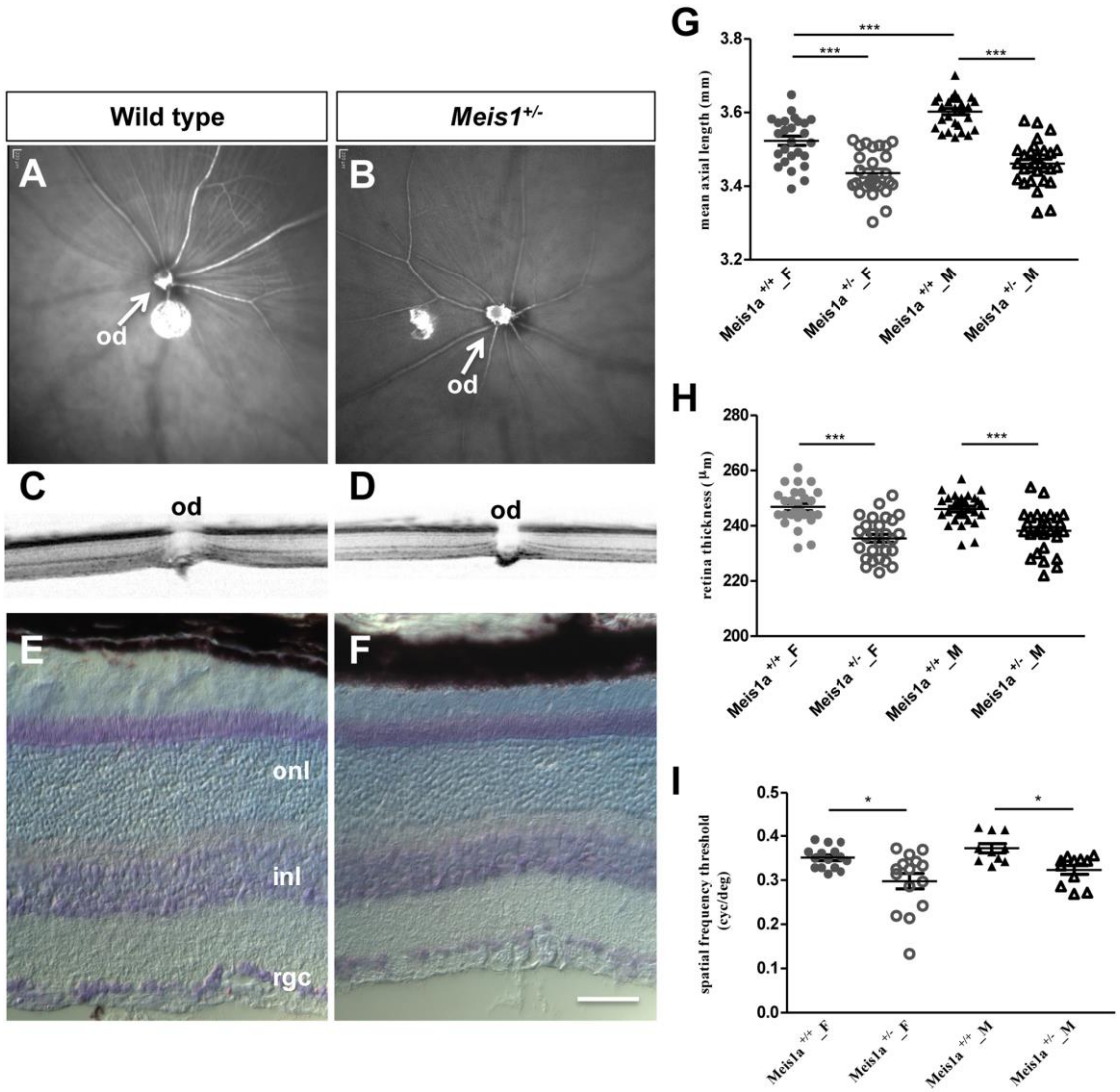

Figure 3. Haploinsufficiency of *Meis1* causes microphthalmic traits in adult mice. A, B) Retina fundus of wt and *Meis1*$^{+/-}$ adult eye obtained by OCT. No difference in the vasculature organization was detected between heterozygous (n=5) and wt (n=5) littermates. C, D) Images of wt and *Meis1*$^{+/-}$ adult central retinas obtained by OCT. E, F) Frontal cryostat sections of wt and *Meis1*$^{+/-}$ adult central retinas stained with cresyl violet. Note the slight difference in thickness of the different layers, leading to an overall reduced thickness of the retina between the two genotypes. G) Eye size measurements by LIB revealed significantly reduced axial eye length in mutants of both sexes: females (F) and males (M) ($p<0.01$); H) Retinal thickness in both females (F) and males (M) was significantly decreased in the *Meis1a*$^{+/-}$. I) Virtual drum vision testing showed a reduced response in both female ($p = 0.012$) and male mutants ($p = 0.01$). Error bars are standard error of the means of n=15 mice per group. *P<0.05. **P<0.01. ***P<0.001. Abbreviation: od, optic disc; onl, outer nuclear layer; inl, inner nuclar layer; rgc, retina ganglion cells. Scale bar, 25μm.

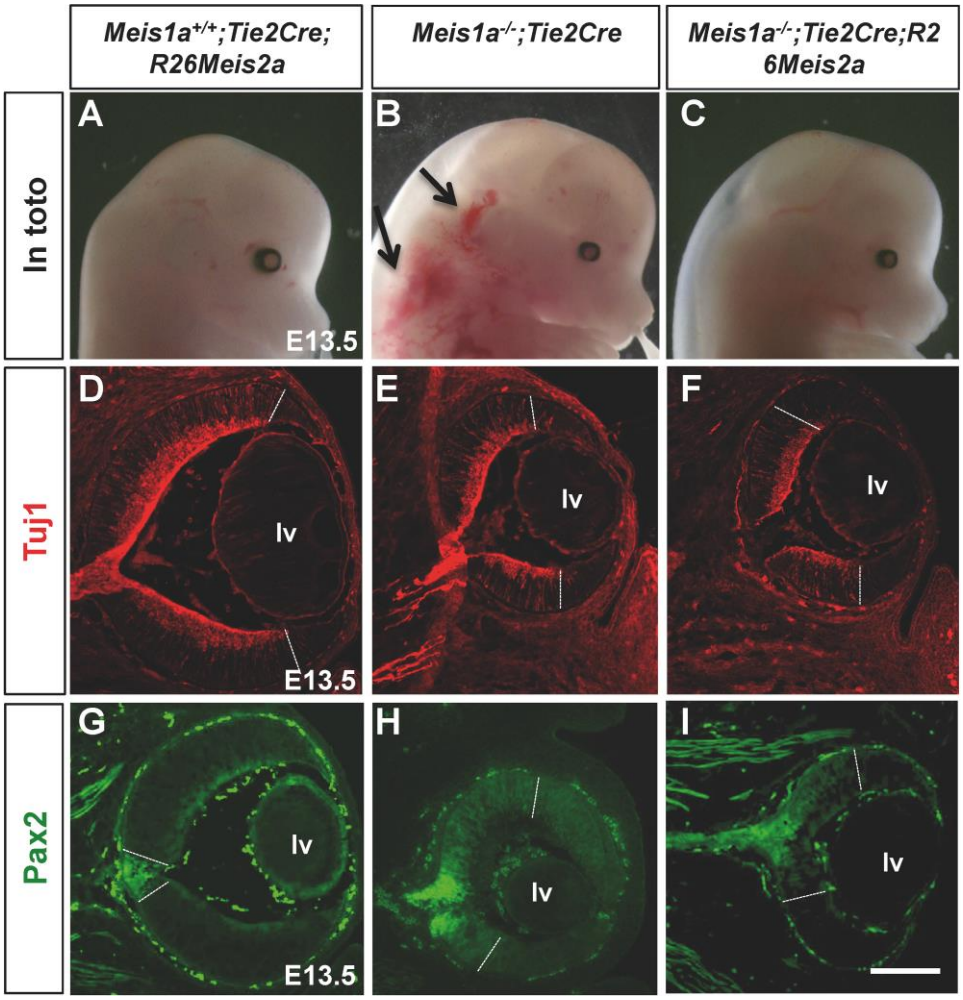

Figure 4. Microphthalmia is not linked to *Meis1* function in the hematopoietic/vascular system. A-C) In toto lateral view of E13.5 *Meis1a*$^{+/+}$*;Tie2Cre;R26Meis2a*; *Meis1a*$^{-/-}$*;Tie2Cre* and *Meis1a*$^{-/-}$*;Tie2Cre;R26Meis2a* embryonic heads. Note that the rescue of the vascular phenotype, characterized by evident haemorrhage (arrows in B) are no longer observed in rescued embryos (C) although the eye size is still reduced in both *Meis1a*$^{-/-}$*;Tie2Cre* and *Meis1a*$^{-/-}$*;Tie2Cre;R26Meis2a* embryos (B, C) as compared to control littermates (A). D-I) Frontal cryostat sections of the optic cup of *Meis1a*$^{+/+}$*;Tie2Cre;R26Meis2a*; *Meis1a*$^{-/-}$*;Tie2Cre* and *Meis1a*$^{-/-}$*;Tie2Cre;R26Meis2a* immunostained with antibodies against Tuj1 and Pax2. Note that the rescue of Meis1a expression in the vasculature does not improve neuronal differentiation and optic cup patterning defects. Dotted lines in the different panels delineate the extent of marker labelling. Abbreviations: lv, lens vesicle; od, optic disc. Scale bar, 25µm

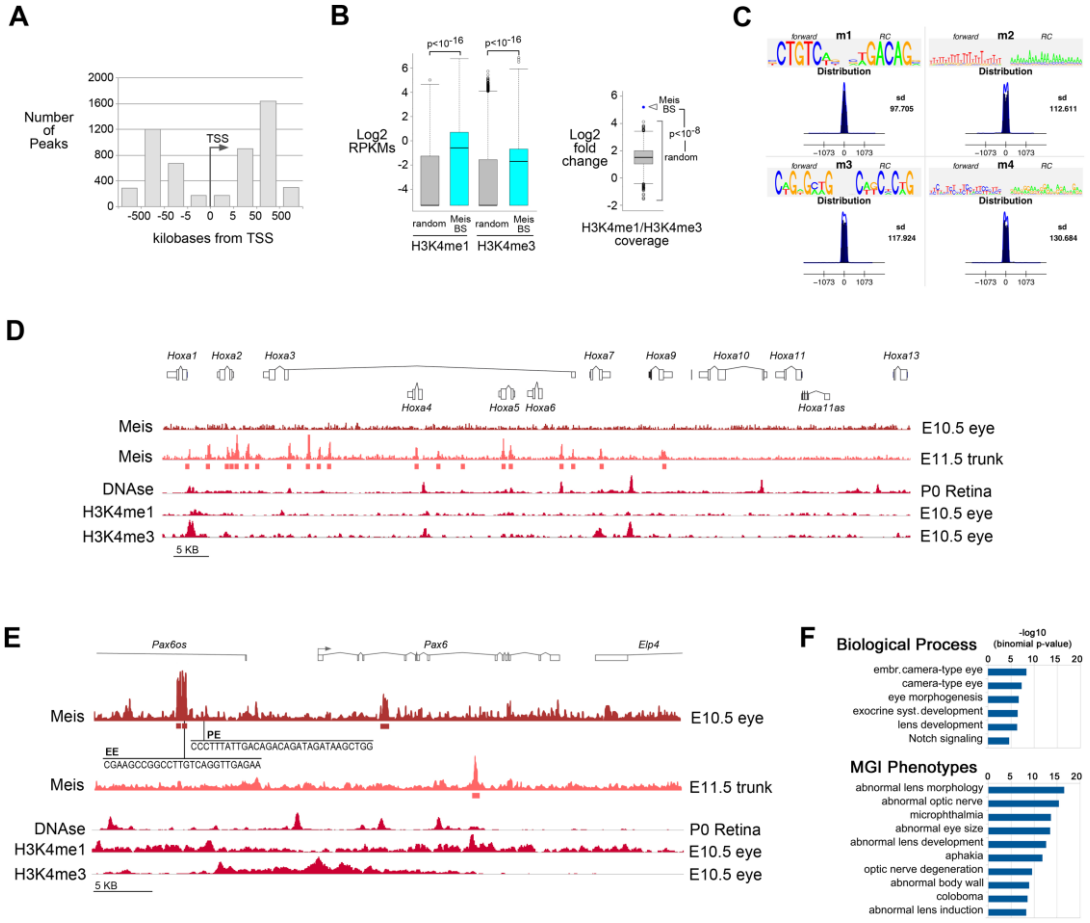

Figure 5. ChIP-seq analysis of Meis1 function in the developing eye. A) Distribution of Meis1-BS by their position with respect to their nearest Transcription Start Site (TSS; GREAT analysis see METHODS). B) Left, distribution of H3K4me1 and H3K4me3 coverage in Meis BS compared with that in a collection of randomly chosen equivalent genomic DNA segments. Right, comparison of H3K4me1/H3K4me3 coverage ratio in Meis BS (blue dot) versus the distribution of the same parameter calculated in a series of randomly chosen equivalent genomic DNA segments. C) *de novo* identification of consensus sequences in the Meis-BS. Four motifs were identified (m1-m4). Forward and reverse complementary (RC) sequences and a graph with the distribution of the positions relative to BS center are shown for each motif. D, E) Representation of the *HoxA* complex and *Pax6* genomic regions showing the Meis1 ChIP-seq read profile from E10.5 eye and E11.5 trunk (Penkov et al., 2013); the P0 DNAse-seq profile (from the ENCODE project; GEO:GSM1014188; (2012), and the H3K4me1 and H3K4me3 ChIP-seq profiles. Detected Meis1-BSs are shown by boxes below the read profiles. E) The sequences bound by Meis in the ectoderm (EE) and pancreatic (PE) enhancers (Zhang et al., 2002; Zhang et al., 2006) are indicated in the eye ChIPseq profile of the *Pax6* genomic region. F) "Biological Process" and "MGI Phenotypes" overrepresented GO classes are shown in order of significance by their Binomial p-value.

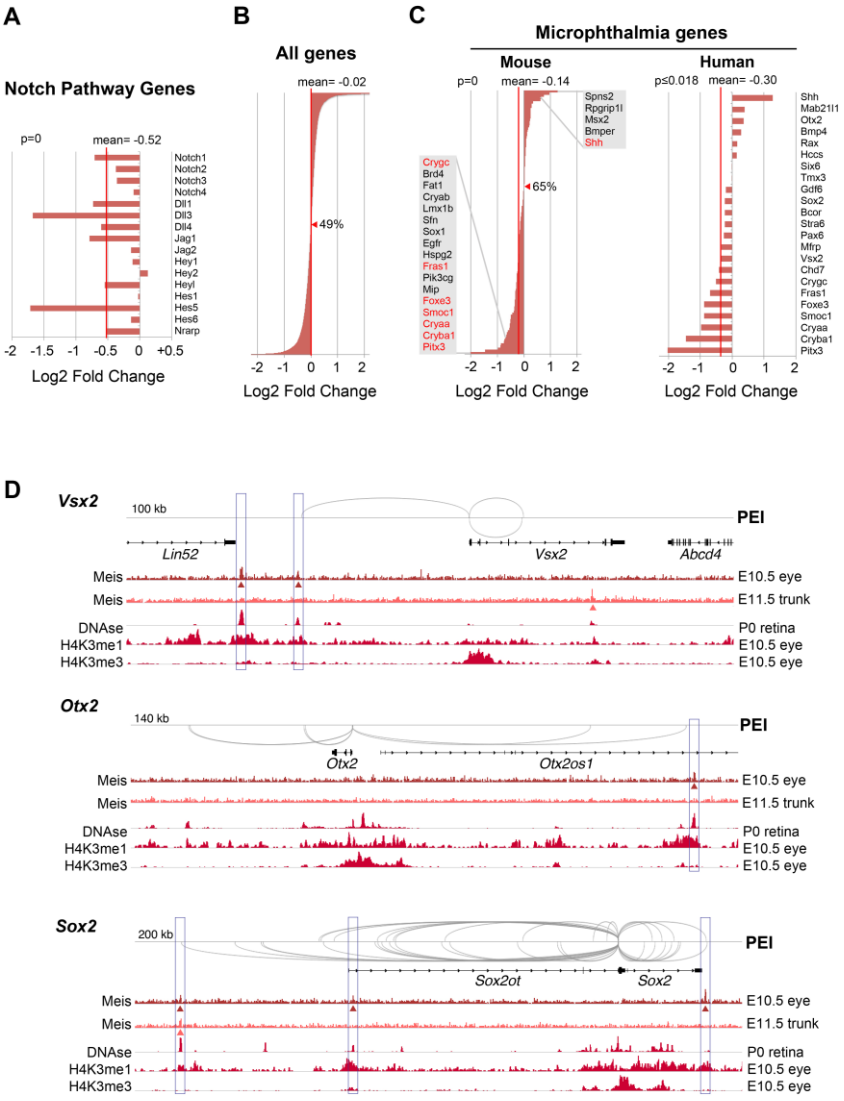

Figure 6. Meis1 regulates components of the Notch signalling pathway and genes involved in microphthalmia. A) The graph shows RNAseq expression level changes in genes encoding the core components of the Notch signalling pathway detected in E10.5 *Meis1*$^{-/-}$ versus wt eyes. B, C) Representations of changes in gene expression detected in *Meis1*$^{-/-}$ for all genes (B), mouse microphthalmia genes and mouse orthologs of human microphthalmia genes (C). Genes are ordered according to their expression change. A red line indicates the mean of expression variations. Grey boxes in C indicate genes with a Log2 fold change > ± 0.5. Genes highlighted in red indicate those whose human ortholog is associated with microphthalmia. The complete list of mouse orthologs of human genes analysed in C is shown on the right of the graph. "p" in A, C indicates the familywise error rate. D) Representation of the *Vsx2*, *Otx2* and *Sox2* genes showing their described Promoter-Enhancer Interactions (PEI) according to Shen et al. (Shen et al., 2012); the Meis1 ChIP-seq read profile

from E10.5 eye and E11.5 trunk (Penkov et al., 2013); the P0 DNAse-seq profile (from the ENCODE project; GEO:GSM1014188; (2012), and the H3K4me1 and H3K4me3 ChIP-seq profiles. Detected Meis1-BS are shown by arrowheads below the read profiles. Boxes highlight the E10.5 eye Meis-BS regions and their coincidence with Histone modification marks and described enhancer-promoter interactions.

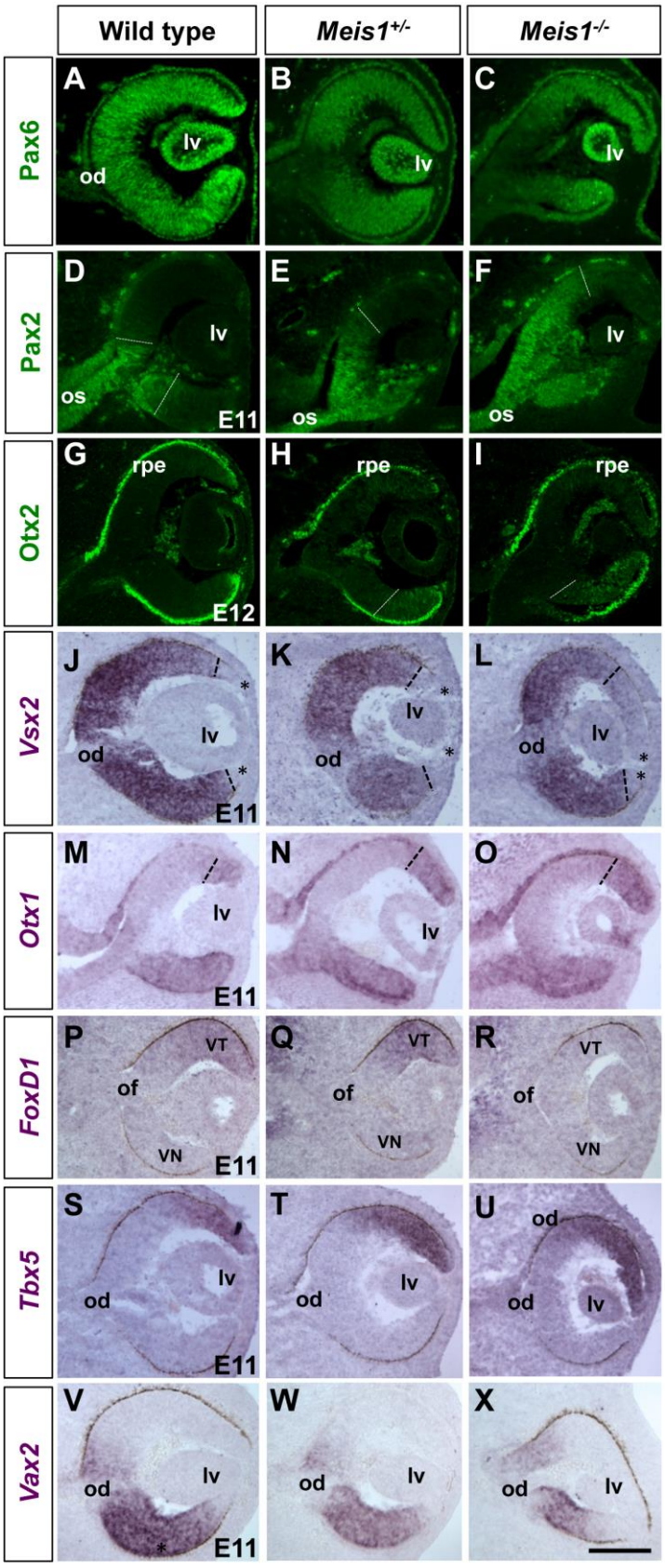

Figure 7. ***Meis1*** **is required to define proper patterning of the optic cup along its principal axes. A-X**) Frontal (A-O,S-X) and horizontal (P-R) cryostat sections of E11 wt,

Meis1$^{+/-}$ and *Meis1*$^{-/-}$ optic cups processed for the markers indicated in the panels. Note the allele-dependent expression-shift of the different markers in *Meis1* mutant optic cups. Dotted lines delineate the extent of marker staining. Abbreviations: lv, lens vesicle; od, optic disc; of, optic fissure; os, optic stalk; rpe, retina pigmented epithelium; VN, ventro-nasal; VT, ventro-temporal. Scale bar, 25 μm.